Twisting Signals for Joint Radar-Communications

Kumar Vijay Mishra

ELLIIT Focus Period Symposium

Linköping University, Sweden

23 April 2026

INDIAN INSTITUTE OF SCIENCE
भारतीय विज्ञान संस्थान

UNIVERSITY OF MARYLAND

DEVCOM ARMY RESEARCH LABORATORY

- NJTech: Wanghan Lv
- ARL/UT Austin: Brian M. Sadler
- UIS Colombia: Henry Arguello, Edwin Vargas, Roman Jacome, Jonathan Arley
- Rice: Ashutosh Sabharwal, West Chen, Nate Raymondi, Kris Li
- IIT Delhi: Arpan Chattopadhyay, Himali Singh

DEVCOM ARMY RESEARCH LABORATORY

The National Academies of SCIENCES ENGINEERING MEDICINE

Research was sponsored by the Army Research Laboratory and was accomplished under Cooperative Agreement Number W911NF-21-2-0288. The views and conclusions contained in this document are those of the authors and should not be interpreted as representing the official policies, either expressed or implied, of the Army Research Laboratory or the U.S. Government. The U.S. Government is authorized to reproduce and distribute reprints for Government purposes notwithstanding any copyright notation herein.

Characteristics of Electromagnetics Waves

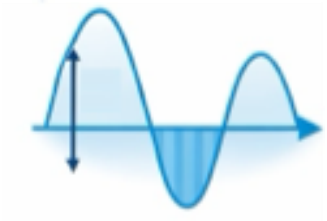

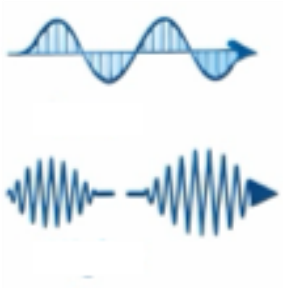

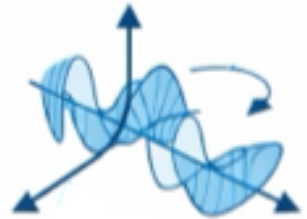

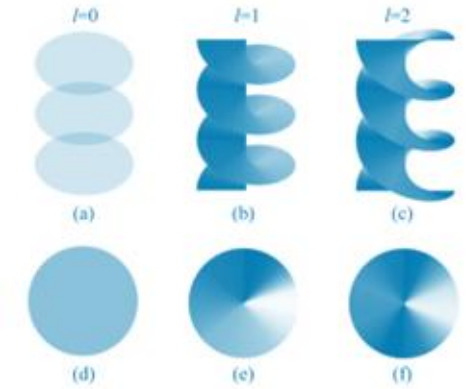

Amplitude

Frequency

Polarization (Spin Angular Momentum)

Orbital Angular Momentum

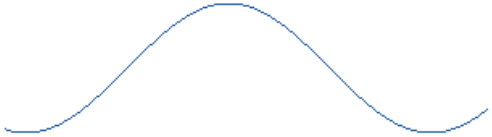

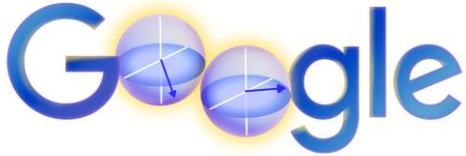

World Quantum Day
(14 April 2026)

SAM is independent of OAM

1 UNPOLARIZED–UNTWISTED
(No SAM, No OAM)

EXAMPLE:
Sunlight

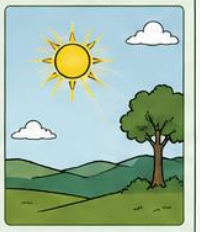

Sunlight is randomly polarized
and has planar wavefronts.

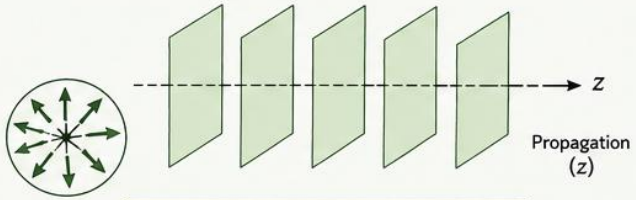

Random polarization (no preferred direction).
Wavefronts are planar (no twist).

2 POLARIZED–UNTWISTED
(SAM ≠ 0, OAM = 0)

EXAMPLE:
GPS signal
(Right-hand
circularly
polarized)

Electric field rotates in time (circular polarization).
Wavefronts are planar (no twist).

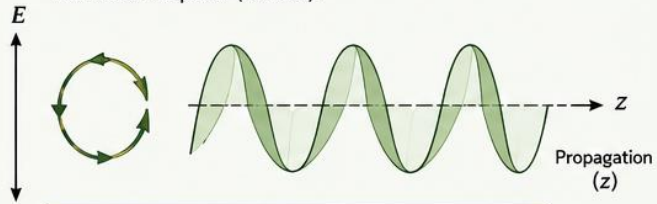

Circular polarization (rotating electric field).
Carries spin angular momentum (SAM ≠ 0), but no OAM.

3 UNPOLARIZED–TWISTED (OAM)
(No SAM, OAM ≠ 0)

EXAMPLE:
Microwave beam
with OAM
(unpolarized)

No preferred polarization, but the phase
has a helical (twisted) structure.

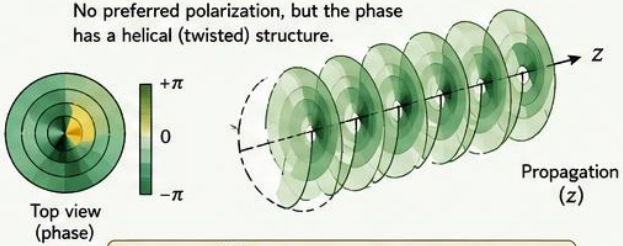

Phase $\propto e^{jl\phi}$ (helical). No fixed polarization.
Carries orbital angular momentum (mode index $l \neq 0$).

4 POLARIZED–TWISTED (OAM + SAM)
(SAM ≠ 0, OAM ≠ 0)

EXAMPLE:
Circularly polarized
vortex beam
(optical OAM
mode)

Electric field is circularly polarized
and the phase is helical.

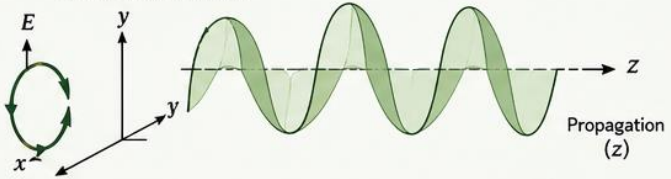

Circular polarization (SAM ≠ 0) and helical phase (OAM ≠ 0).
Carries both spin (SAM) and orbital (OAM) angular momentum.

OAM History

Foundations in physics
Angular momentum in quantum systems

1930s
Conceptual roots in atomic physics and the quantization of angular momentum.

Discovery of optical vortices
Phase singularities and structured light

1970s–80s
Optical vortices and phase singularities (Nye and Berry).

1992 Physical Review A
Les Allen et al. show that OAM is independent of spin angular momentum (SAM).

Applications in communications and sensing
From free-space links to radar systems

2014
Twisted light sends images across Vienna.
nature

2016
Physicists twist light, send 'Hello World' message between islands.
SCIENTIFIC AMERICAN

2018
NTT demonstrates 100 Gbps wireless transmission using OAM multiplexing for the first time.
Microwave Journal

Quantum structured light
OAM in quantum states and experiments

2018
Nobel Prize in Physics — optical tweezers and optical manipulation.

2022
Nobel Prize in Physics — OAM states of photons used in quantum experiments.

2023
Nobel Prize in Physics — attosecond pulses for ultrafast probing of OAM physics.

Emerging frontiers
From visualization to biomedical impact

2024
OAM-based optical techniques poised to transform medical diagnostics and imaging.
PHYS.ORG

1930 1970 1990 2010 2020 2024+

Historical Notes

Different OAM modes are mutually orthogonal ⟶ New way to achieve orthogonality

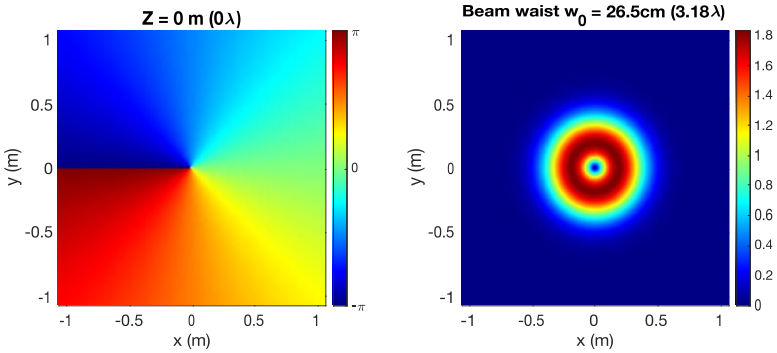

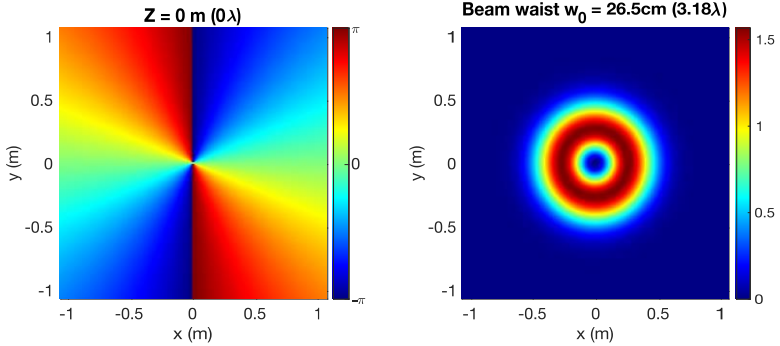

$$\int_0^{\infty}\int_0^{2\pi} LG(r,\phi,z;l_1,p_1)\,LG^{*}(r,\phi,z;l_2,p_2)\,d\phi\,dr = \begin{cases} 0 & \text{if } l_1 \neq l_2 \text{ or } p_1 \neq p_2 \\ 1 & \text{if } l_1 = l_2 \text{ and } p_1 = p_2 \end{cases}$$

Outline

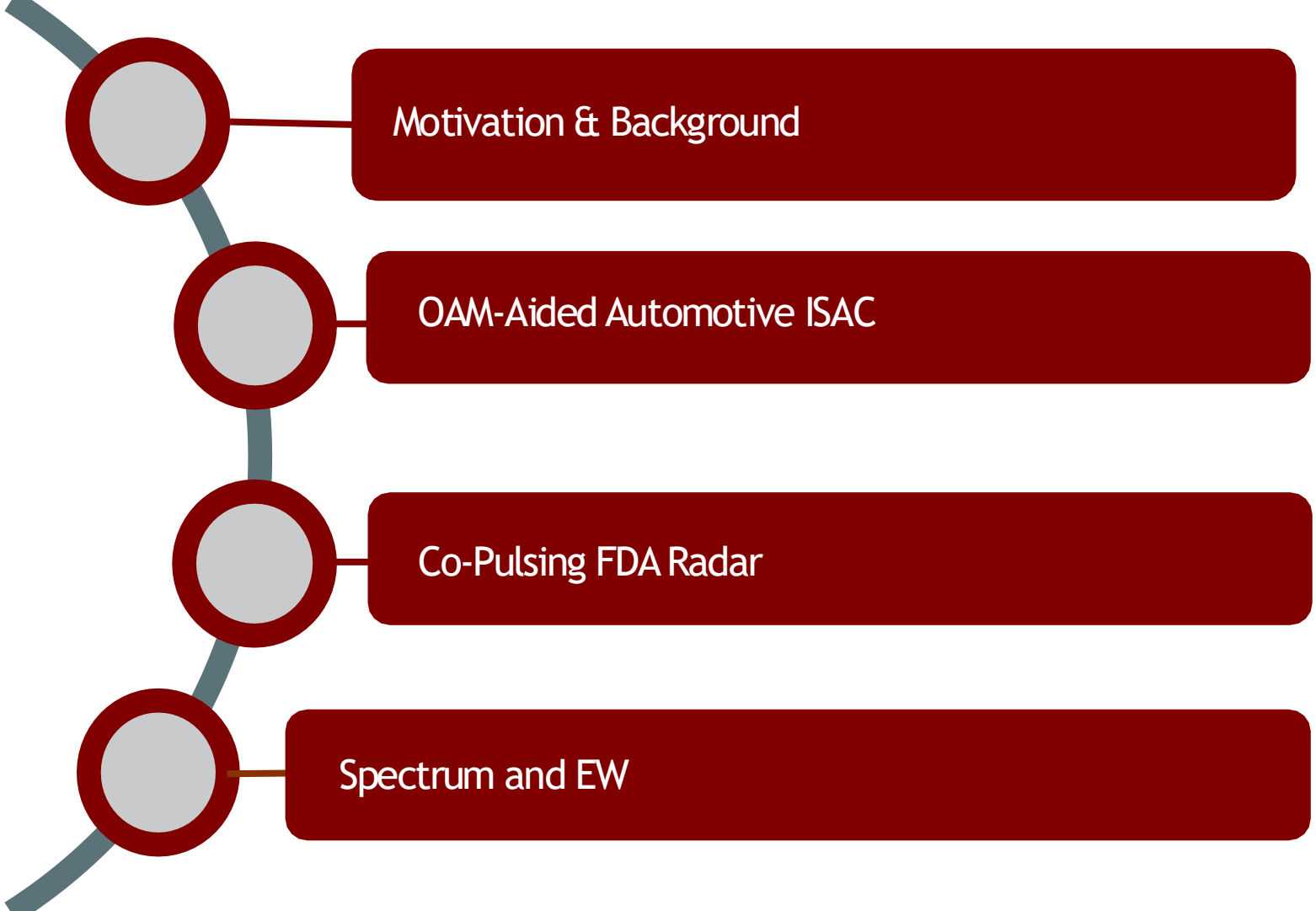
Motivation & Background
OAM-Aided Automotive ISAC
Co-Pulsing FDA Radar
Spectrum and EW

Courtesy: Stranger Things (S05E01)

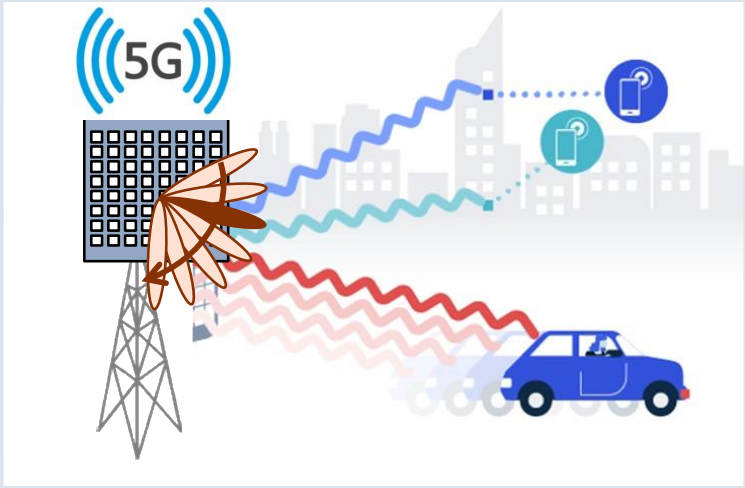

Laguerre-Gaussian Beams

Which Beam to Use?

- Laguerre–Gaussian (LG) Vortex Beam: Easy to generate via metasurfaces
  - Beam waist w_0 (determines $w(z)$): no clear guideline

Describes amplitude

$$E_{\{l,p\}}(r,z,\phi) = \sqrt{\frac{2p!}{\pi(p+|l|)!}}\ \frac{1}{w(z)}\left(\frac{r\sqrt{2}}{w(z)}\right)^{|l|}\exp\left(\frac{-r^2}{w^2(z)}\right)L_p^{|l|}\left(\frac{2r^2}{w^2(z)}\right)$$

$$\exp\left(\frac{-i\,k_0 r^2 z}{2(z^2+z_R^2)}\right)\exp\left(-il\phi + i(2p+|l|+1)\arctan\left(\frac{z}{z_R}\right)\right)$$

Describes phase

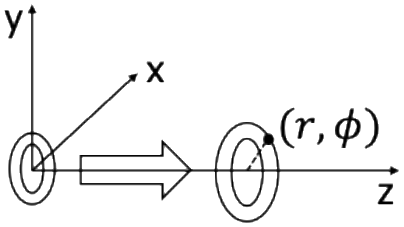

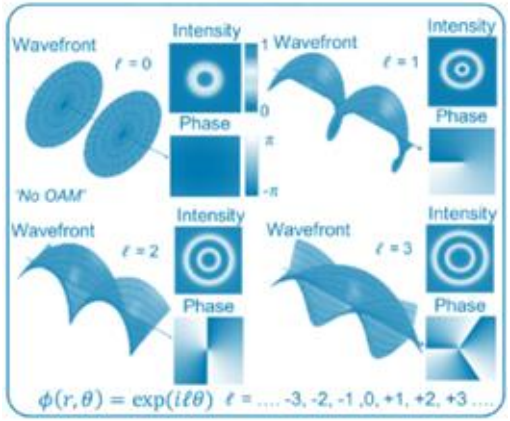

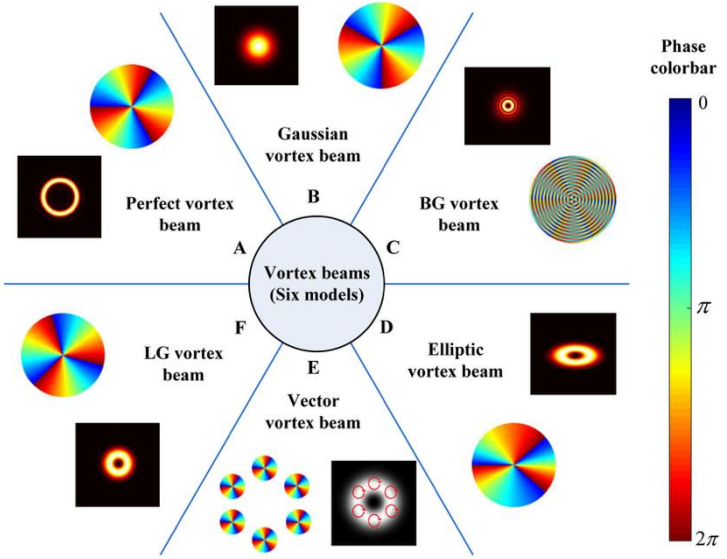

W Lv, KV Mishra, J Hu, "Twisting Signals for Joint Radar-Communications: An OAM Vortex Beam Approach." IEEE T-AP, 2026

OAM Modes for Different *p* and *l*

Azimuthal index l	Radial index $p \rightarrow$	$p = 0$	$p = 1$	$p = 2$	$p = 3$
$l = 0$	Intensity				
	Phase	 constant ($l = 0$)	 constant ($l = 0$)	 constant ($l = 0$)	 constant ($l = 0$)
$l = 1$	Intensity				
	Phase				
$l = -1$	Intensity				
	helical (−1)				
$l = 2$	Intensity				
	helical (+2)				

L-G Beams may not be Ideal!

- L-G Beams are susceptible to turbulence and interference
- OAM modes encode azimuth but no range information
- Solution: Use Frequency-Diverse Arrays (FDAs)

Phased Array (PA)

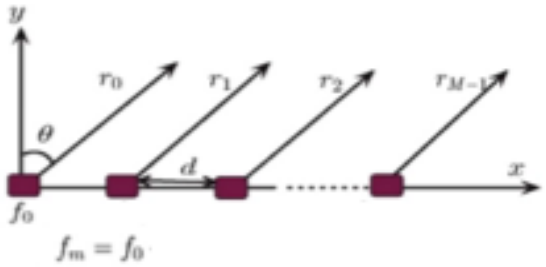

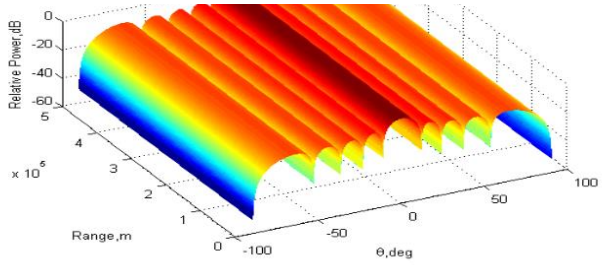

Angle-Dependent Beampattern

Frequency Diverse Array (FDA)

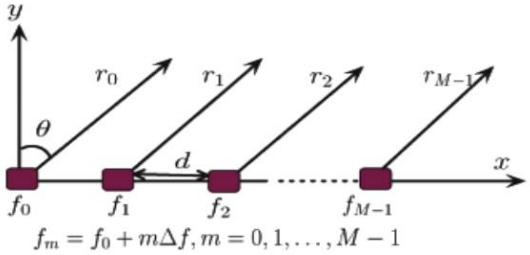

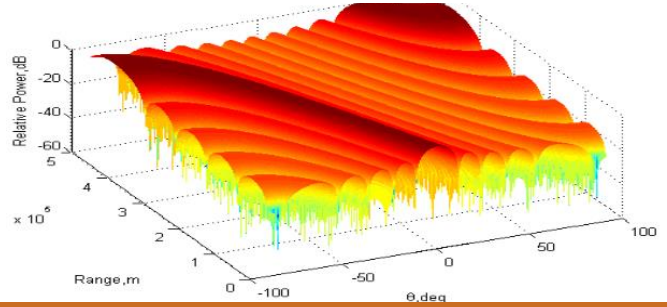

Range-Angle-Dependent Beampattern

… but in classical far-field!

Courtesy: Species II (1998)

Signal Processing

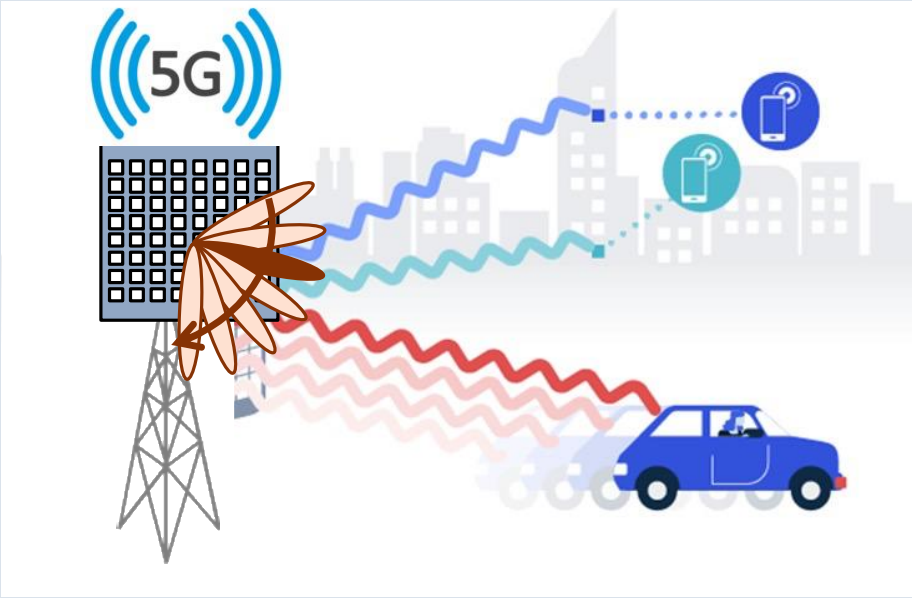

Bistatic OAM-FDA ISAC

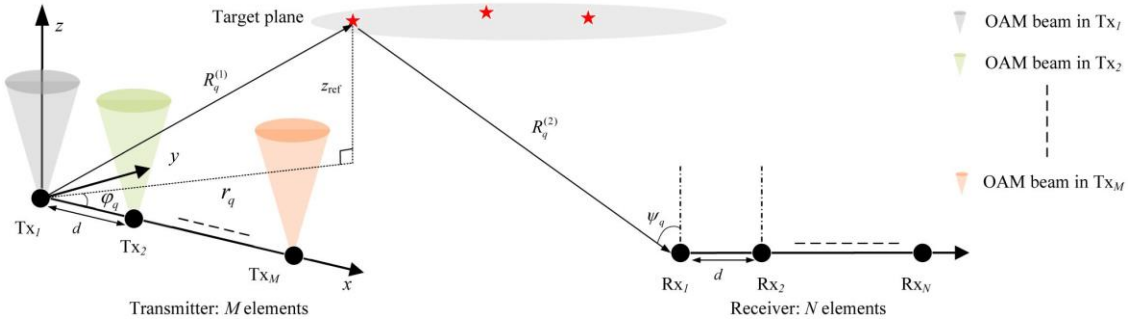

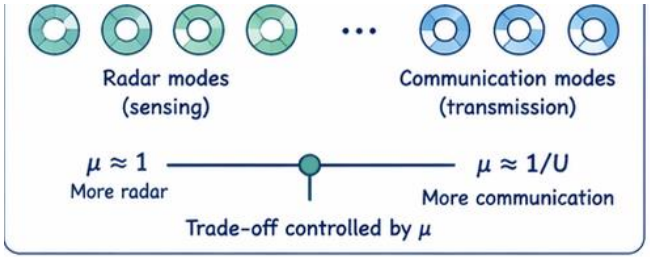

1. TRANSMIT SIGNAL

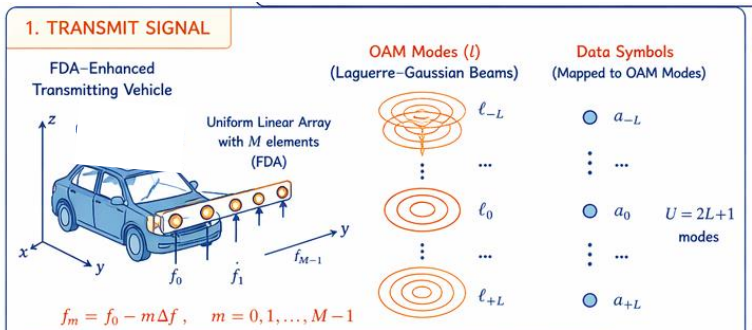

Transmit signal from m-th antenna for mode ℓ_u :

$$s_{\ell_u,m}(t) = a_u \; e^{j2\pi f_m t}, \quad m = 0, 1, \ldots, M-1, \quad u = -L, \ldots, L$$

2. CHANNEL MODEL

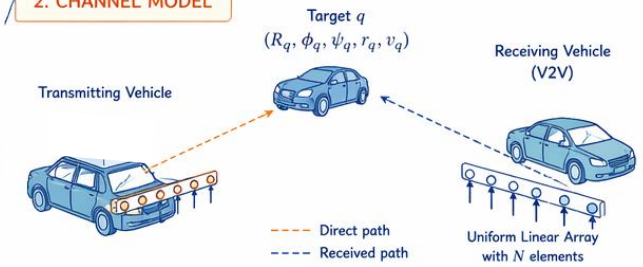

Physical Meaning
- R_q : Range
- ϕ_q : Azimuth (DoD)
- ψ_q : Azimuth (DoA)
- r_q : Radial distance
- v_q : Radial velocity

Baseband signal at receiver for mode ℓ_u :

$$x_{\ell_u}(t) = \sum_{q=1}^{Q} \underbrace{\tilde{\rho}_q(t)}_{\text{Propagation gain}} \; a_u \; \underbrace{e^{j\Phi_{\ell_u q}}}_{\text{OAM-dependent phase}} \; \underbrace{\mathbf{b}(R_q)}_{\text{Range steering (FDA)}} \otimes \underbrace{\mathbf{a}_R(\psi_q)}_{\text{Angle steering (ULA)}} + \underbrace{\mathbf{n}(t)}_{\text{Noise}}$$

OAM-dependent phase

$$\Phi_{\ell_u q} = -\pi \frac{r_q^2 - r_{max}}{\lambda_0 R_\ell} - \ell_u \, \phi_q$$

W Lv, KV Mishra, J Hu, “Twisting Signals for Joint Radar-Communications: An OAM Vortex Beam Approach.” IEEE T-AP, 2026

Range and Angle Estimation

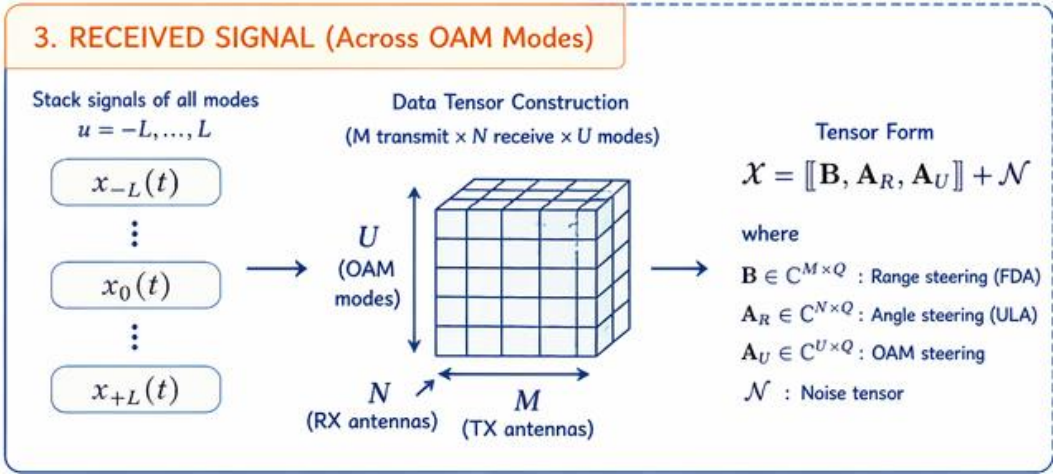

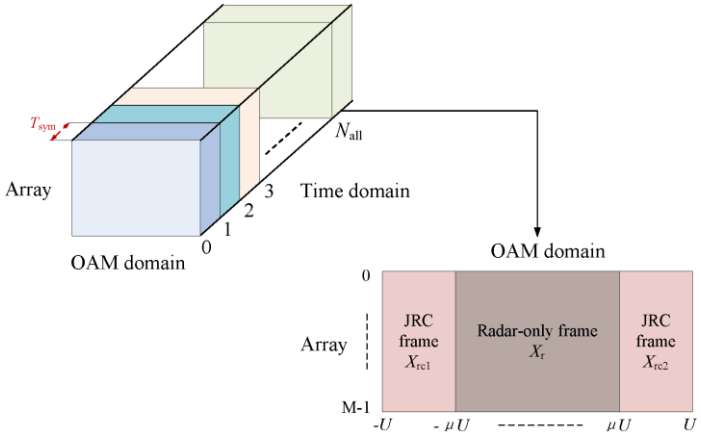

Range-Azimuth-DoA estimation:

- FDA structure allows auto-pairing of bistatic range and angles

Doppler and Comms Estimation

- **Doppler estimation: Take the derivative of phase and convert the angular frequency to Doppler velocity**
- **Use MRC to**

1 Build slow-time data cube

Collect M pulses: $y_m(t), \quad m = 0, \ldots, M-1$

After steps in III.A, obtain OAM–range–angle bin for each target (R_k, ψ_k, ϕ_k).

Form slow-time sequence:

$$z_k[m] = Y_{lk}(R_k, \psi_k, \phi_k; m), \quad m = 0, \ldots, M-1$$

2 Doppler FFT

$$Z_k[\nu] = \sum_{m=0}^{M-1} z_k[m]\, e^{-j2\pi\nu m/M}$$

Peak at $\nu_k \quad \Rightarrow \quad v_k = \dfrac{\lambda\, \nu_k}{2}$

3 Rotational velocity (from OAM phase evolution)

The phase of $z_k[m]$ contains a rotational Doppler term due to OAM:

$$z_k[m] \approx A_k\, e^{j(2\pi f_{D,k} T_r m + l_k \omega_k T_r m + \varphi_{0,k})}$$

Unwrap phase $\angle z_k[m] = \beta_k m + \varphi_{0,k}$

$$\Rightarrow \quad \omega_k = \frac{\beta_k - 2\pi f_{D,k} T_r}{l_k T_r}$$

- T_r : pulse repetition interval
- $f_{D,k} = \dfrac{2v_k}{\lambda}$
- ω_k : rotational velocity (rad/s)

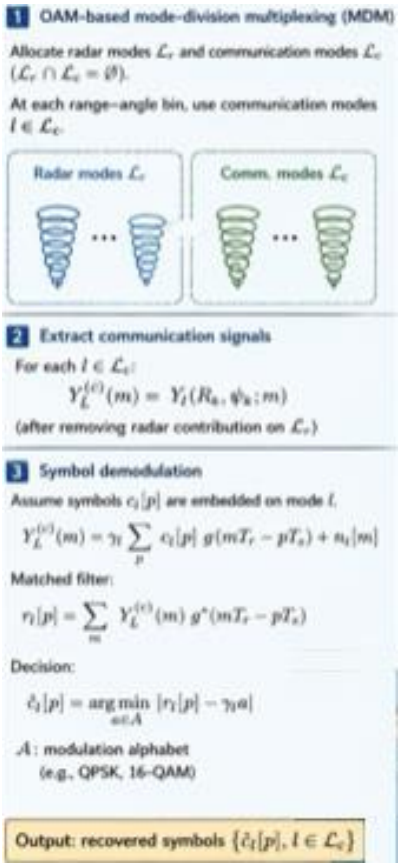

W Lv, KV Mishra J Lu "Multiplexing for Joint Radar-Communications: An OAM Vortex Beam Approach." IEEE T-AP, 2026

Courtesy: The Midnight Sky (2020)

Performance Guarantees

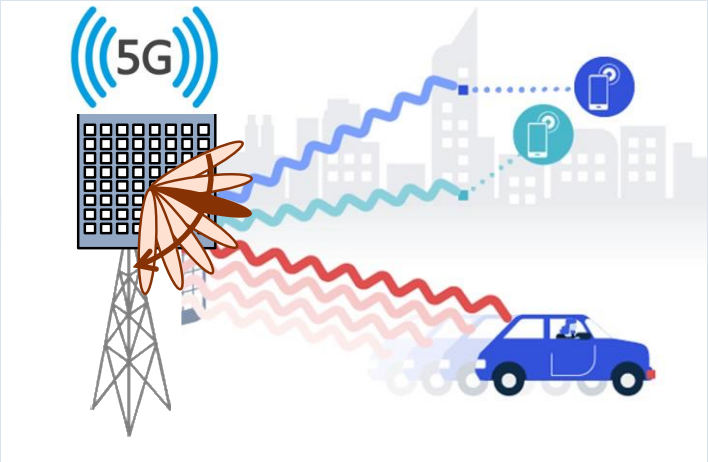

Provable Guarantees using Kruskal Rank

Theorem [Lv, Mishra, Hu 2026]

Consider a bistatic FDA system with an M(N)-element transmit (receive) ULA and d, Δf be the interelement spatial spacing and frequency increment, respectively. Each transmit element sends out a total of 2U+1 OAM states with the inter-state spacing δ. Assume that there are Q scatterers with R_{max} being the maximum bi-static range and the JRC sharing factor is denoted as μ. If

$$\begin{aligned}
&\textbf{C1}\ \ d \leq \tfrac{c}{2f_0},\\
&\textbf{C2}\ \ \Delta f \leq \tfrac{c}{R_{\max}},\\
&\textbf{C3}\ \ N > Q,\\
&\textbf{C4}\ \ M > Q,\\
&\textbf{C5}\ \ \tfrac{1}{U} \leq \mu \leq 1,
\end{aligned}$$

then the unknown parameters of Q scatterers and communication symbols a_u can be perfectly recovered from the multiplexing covariance matrix **R**.

W Lv, KV Mishra, J Hu, "Twisting Signals for Joint Radar-Communications: An OAM Vortex Beam Approach." IEEE T-AP, 2026

Detection Performance

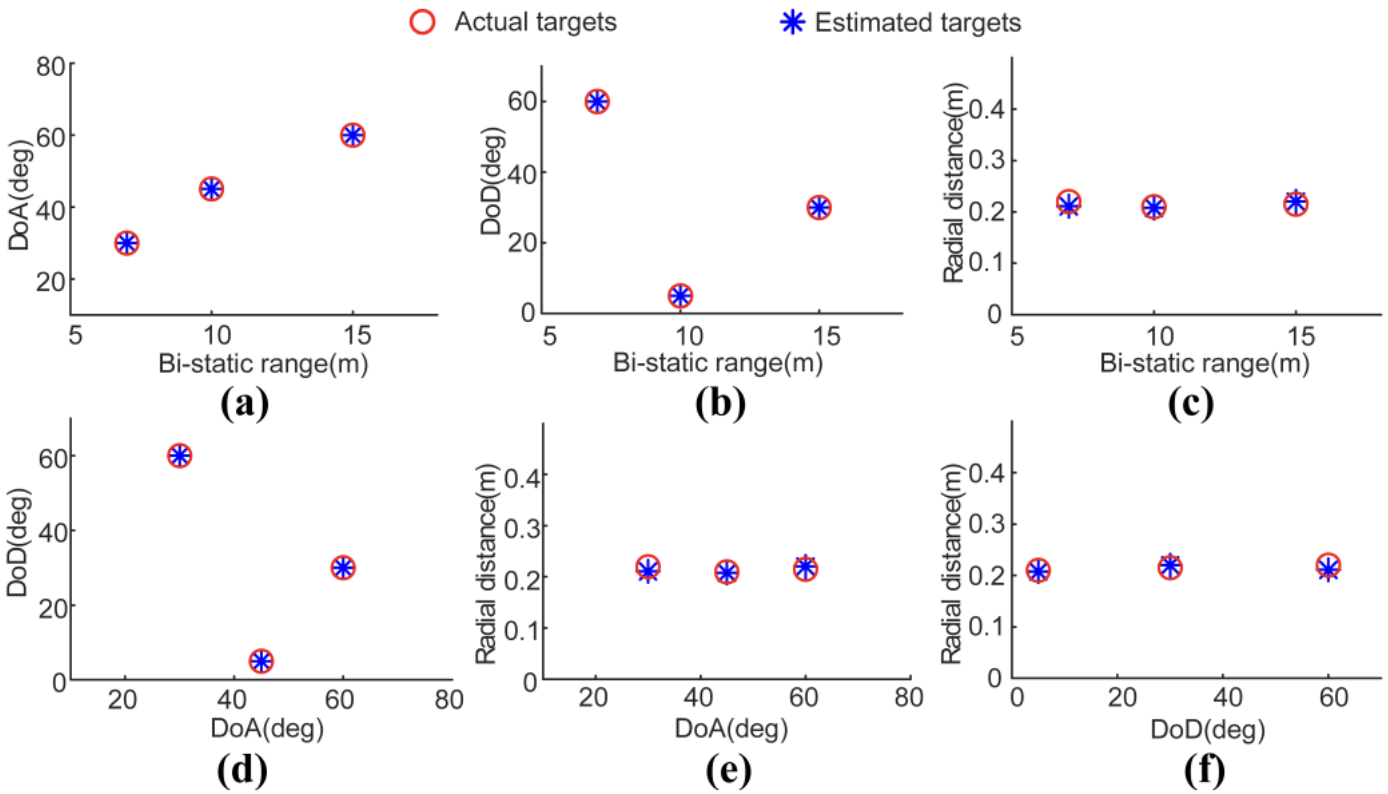

W Lv, KV Mishra, J Hu, "Twisting Signals for Joint Radar-Communications: An OAM Vortex Beam Approach." IEEE T-AP, 2026

Estimation Performance

CRLBs

Parameter	CRLB (approx.)
Range R_k	$\mathrm{var}(\hat{R}_k) \geq \frac{c^2}{8\pi^2\,\mathrm{SNR}\beta_2}$
DoA ψ_k	$\mathrm{var}(\hat{\psi}_k) \geq \frac{6}{\mathrm{SNR}\,N(N^2-1)(2\pi\Delta f\tau_k)^2}$
Azimuth ϕ_k (OAM)	$\mathrm{var}(\hat{\phi}_k) \geq \frac{1}{\mathrm{SNR}\sum l\in\mathcal{L}_r\, l^2}$
Velocity v_k	$\mathrm{var}(\hat{v}_k) \geq \frac{\lambda^2}{8\pi^2\,\mathrm{SNR}\,T_r^2\sum_m(m-\bar{m})^2}$
Rotational ω_k	$\mathrm{var}(\hat{\omega}_k) \geq \frac{1}{\mathrm{SNR}\,l_k^2\,T_r^2\sum_m(m-\bar{m})^2}$
Complex amp. α_k	$\mathrm{var}(\hat{\alpha}_k) \geq \frac{\sigma^2}{2MN}$

β_2: effective bandwidth factor of $g(t)$, τ_k: delay of target k.

RMSE Compared with CRLB

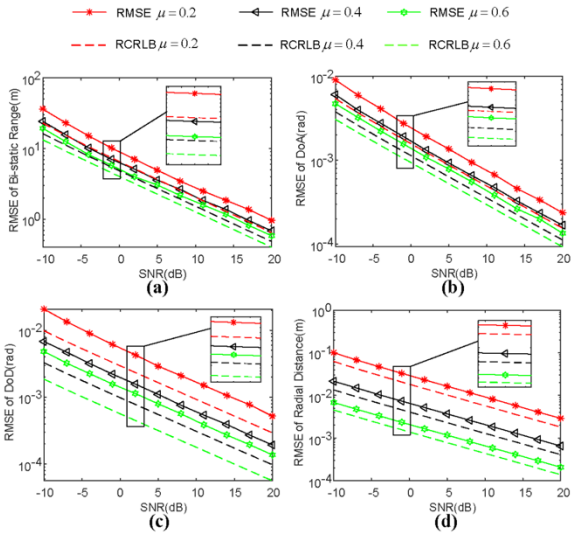

Target RMSE for Various μ

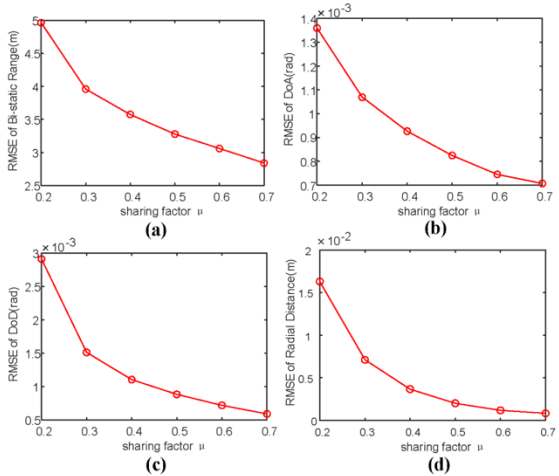

W Lv, KV Mishra, J Hu, "Twisting Signals for Joint Radar-Communications: An OAM Vortex Beam Approach." IEEE T-AP, 2026

Courtesy: Foundation (S01E03)

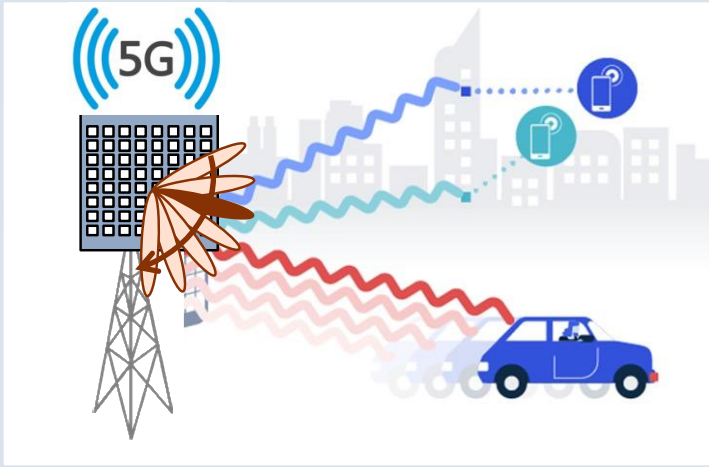

Co-Pulsing FDA Radar

FDA Consumes More Spectrum

Introduction of FOs → Additional Bandwidth

Limited work on Doppler estimation

Solutions:

- Sparse FDA – Fewer elements and FOs
- FOs can be optimized based on available bandwidth
  - Logarithmic [Khan et al., 2014]
  - Non-uniform [Basit et al., 2017]
  - Random [Liu et al., 2016]
  - Co-prime FDA [Qin et al., 2017]
    - Integers that share no common factors except 1: (2,3), (4,9), (6, 10, 15)
  - FDA-MIMO [Sedighi et al., 2019]

Our Approach:

- Fewer FOs → Less bandwidth and more EW tolerance
- Employ FDA to jointly extract range-angle parameters

Co-Pulsing FDA Radar

Array[a]	FO	Spectrum[b]	Beampattern[c]	PRI	Antennas[d]	Pulses[e]
L-shaped ULA (U-U) [35]	None	B	Angle	Uniform	$Q+1$	$Q+1$
L-shaped Co-prime array (C-U) [36]	None	B	Angle	Uniform	$2\sqrt{Q+1}-1$	$Q+1$
L-shaped ULA (U-C)	None	B	Angle	Co-prime	$Q+1$	$2\sqrt{Q+1}-1$
L-shaped Co-prime array (C-C)	None	B	Angle	Co-prime	$2\sqrt{Q+1}-1$	$2\sqrt{Q+1}-1$
L-shaped FDA (U-Cube)	Linear	$B+(P_s-1)\Delta f$	Angle-range	Uniform	$Q+1$	$Q+1$
L-shaped FDA (UUC)	Linear	$B+(P_s-1)\Delta f$	Angle-range	Co-prime	$Q+1$	$2\sqrt{Q+1}-1$
L-shaped FDA (UCU)	Co-prime	$B+\xi_{P_s-1}\Delta f$	Angle-range	Uniform	$Q+1$	$Q+1$
L-shaped FDA (UCC)	Co-prime	$B+\xi_{P_s-1}\Delta f$	Angle-range	Co-prime	$Q+1$	$2\sqrt{Q+1}-1$
L-shaped Co-prime FDA (CUU)	Linear	$B+(P_s-1)\Delta f$	Angle-range	Uniform	$Q+1$	$Q+1$
L-shaped Co-prime FDA (CUC)	Linear	$B+(P_s-1)\Delta f$	Angle-range	Co-prime	$Q+1$	$2\sqrt{Q+1}-1$
L-shaped Co-prime FDA (CCU)	Co-prime	$B+\xi_{P_s-1}\Delta f$	Angle-range	Uniform	$2\sqrt{Q+1}-1$	$Q+1$
L-shaped Co-prime FDA (C-Cube)	Co-prime	$B+\xi_{P_s-1}\Delta f$	Angle-range	Co-prime	$2\sqrt{Q+1}-1$	$2\sqrt{Q+1}-1$

L-shaped array:

- Simpler 2-D FDA structure to perform co-prime sampling in spatial, spectral, and Doppler domains.
- L-shaped previously investigated for ULA [Kishigami et al, 2016] and co-prime array [Elbir, 2020]

W. Lv, K. V. Mishra, and S. Chen, ``Co-pulsing FDA radar," IEEE T-AES, 2023.

Co-Pulsing FDA Radar

CCC Configuration

- Co-Prime Array in L-Shaped Configuration
- Co-Prime Offsets
- Co-Prime Pulsing

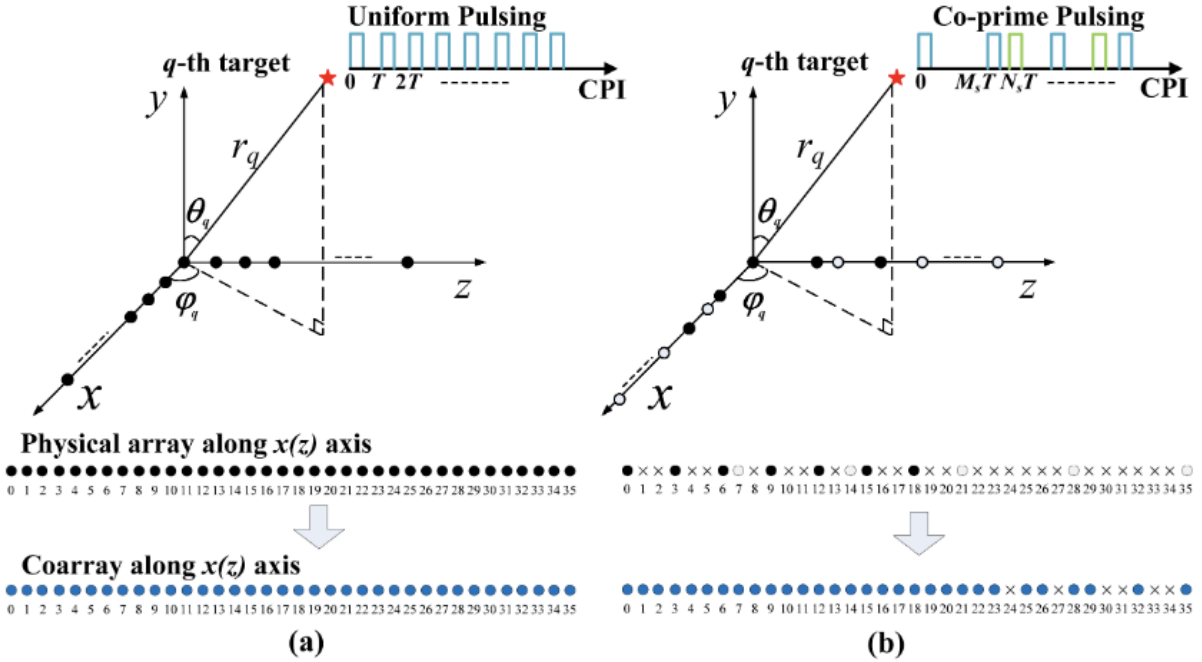

- **Co-Pulsing imparts additional DoFs to sparse FDA design**
- **Extraction of Doppler is coupled with other parameters (second-order statistics)**

W. Lv, K. V. Mishra, and S. Chen, ``Co-pulsing FDA radar," IEEE T-AES, 2023.

C-Cube Auto-Pair*ing* (CCing)

Ipso-Facto Joint Estimation

- Parameter retrieval algorithm employs SVD of the concatenated covariance matrix:
  - Elevation and azimuth embodied in left EVs
  - Range and Doppler embodied in right EVs
- Auto-pairing property between left and right eigenvectors allows for automatic pairing of 2-D DoA with range and Doppler velocity
- Physical reason: L-shaped + FDA structure (range-angle beampattern)
- Kruskal rank properties are used to guarantee the recovery conditions

- Difficult to generalize tensor methods for L-shaped arrays; no auto-pairing
- CCing also works when some target parameters are the same (at the cost of some DoFs)

W. Lv, K. V. Mishra, and S. Chen, ``Co-pulsing FDA radar," IEEE T-AES, 2023.

Co-Pulsing Radar

Range-dependent beampattern: reduce number of pulses, spectrum usage, and antenna elements simultaneously

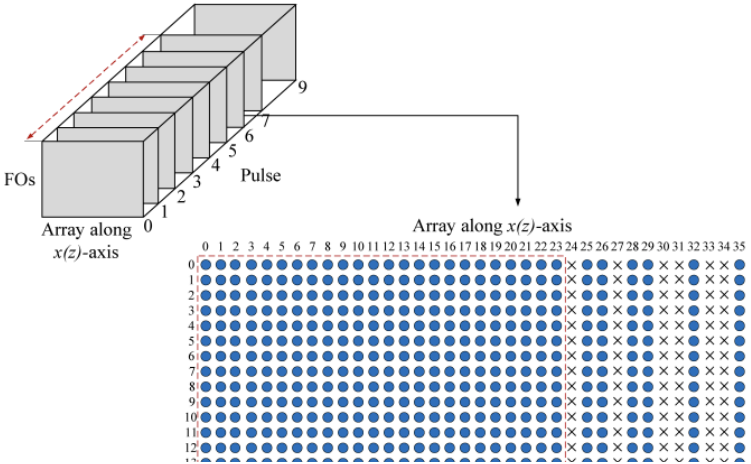

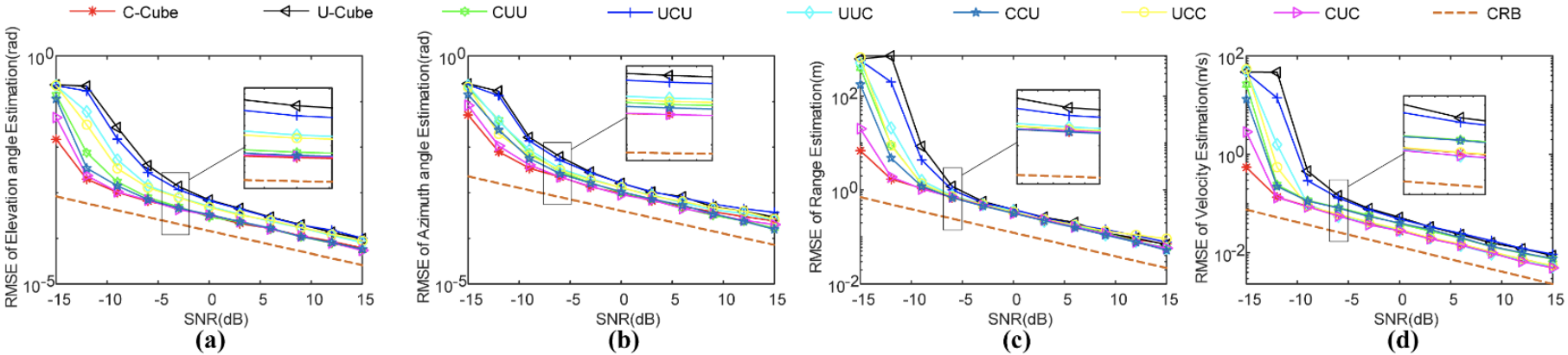

W. Lv, K. V. Mishra, and S. Chen, ``Co-pulsing FDA radar," IEEE T-AES, 2023.

Relationship with Other Arrays

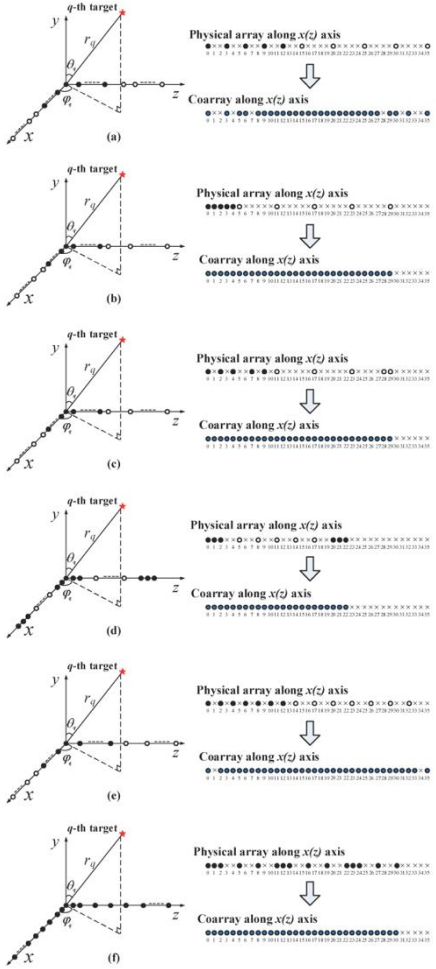

Array	$\mathcal{L}_{\mathrm{H}}$ [a]
L-shaped uniform FDA (U-Cube)	0.76
L-shaped CADiS FDA	0.4302
L-shaped nested FDA	0.6303
L-shaped super-nested FDA	0.5342
L-shaped CNA FDA	0.5859
L-shaped GNA FDA	0.5969
L-shaped multi-coset FDA	0.5985
L-shaped Co-prime FDA (C-Cube)	0.5340

[a] Computed for common physical aperture of $35d$ along each axis.

C-Cube offers a trade-off between high DoFs and mild coupling

A fundamental array structure from which all others could be derived

W. Lv, K. V. Mishra, and S. Chen, ``Co-pulsing FDA radar," IEEE T-AES, 2023.

Courtesy: Independence Day (1996)

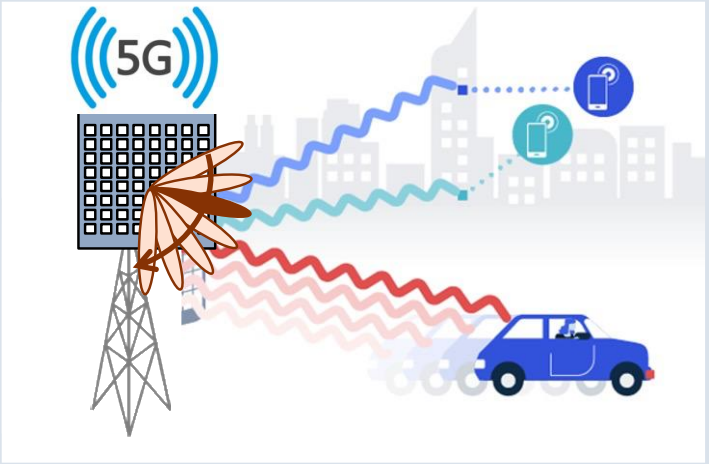

Generalizations

Co-Pulsing Applications

Co-STAP

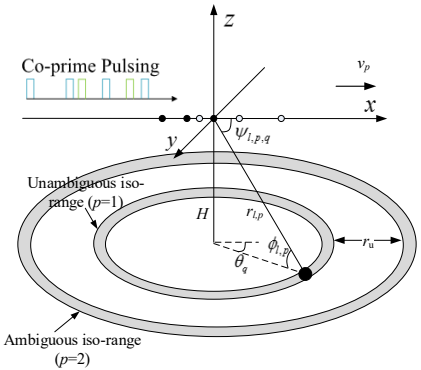

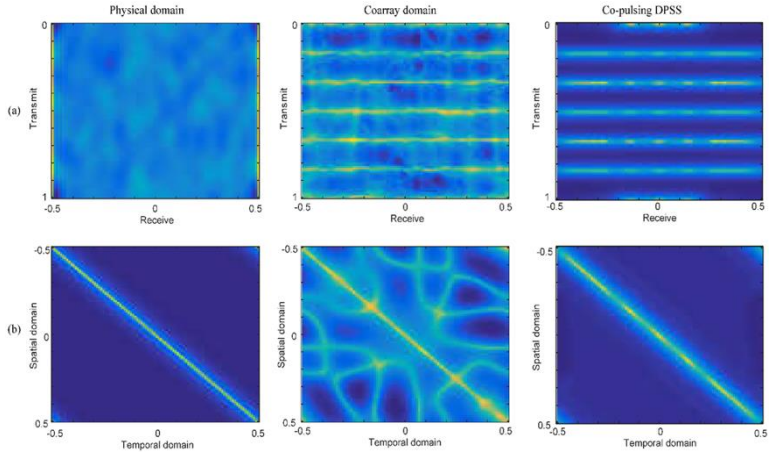

Co-Chirping with FMCW Radar

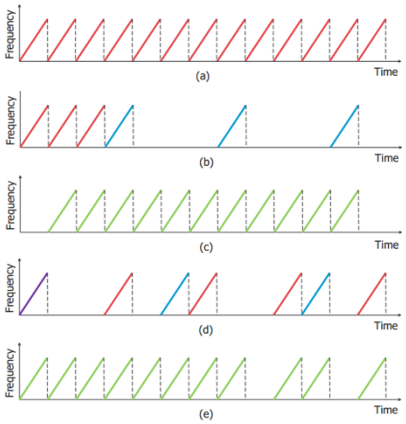

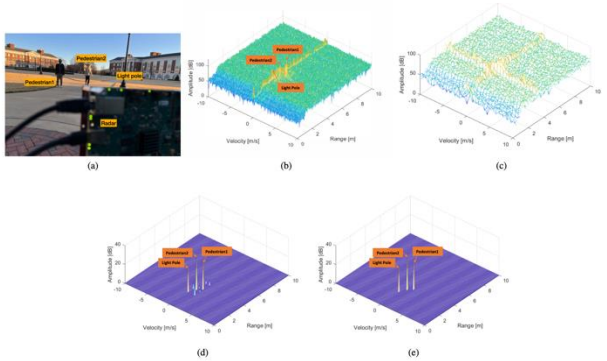

W. Lv and K. V. Mishra, "CoSTAP: Clutter suppression via co-pulsing FDA-STAP," IEEE T-AES, 2024

L. Xu, S. Sun, K. V. Mishra, and Y. D. Zhang, "Automotive FMCW radar with difference co-chirps," IEEE T-AES, 2023.

Courtesy: Top Gun: Maverick (2022)

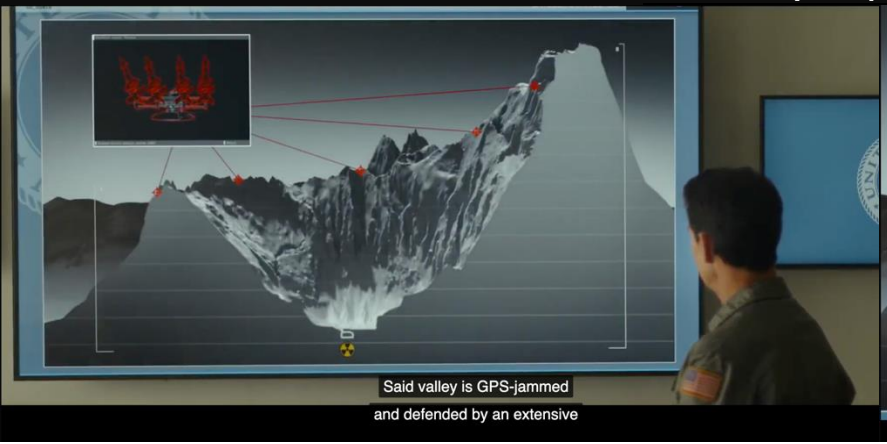

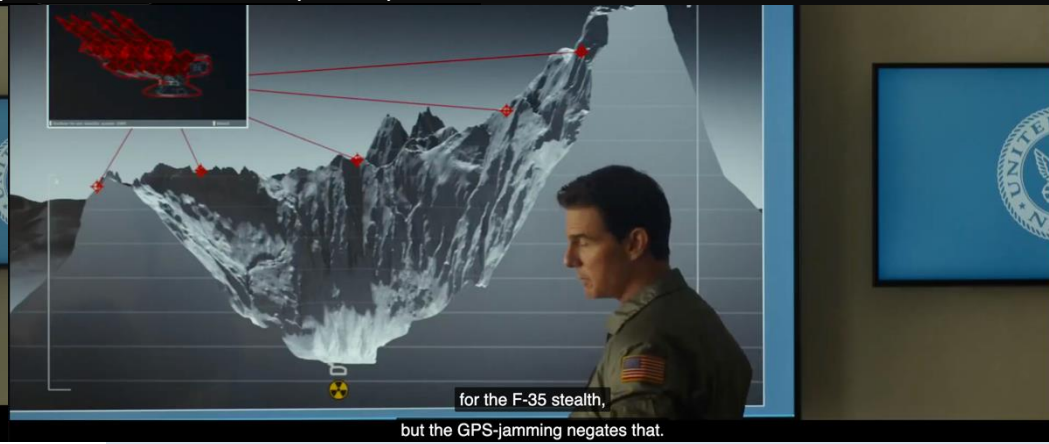

Spectrum and EW

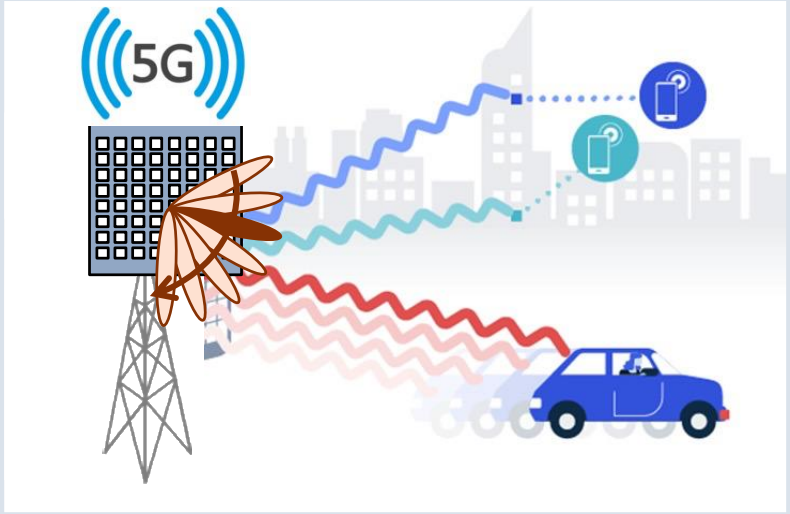

Understanding Spectrum Congestion is Essential in Modern Warfare

Science THE WIRE

Ukraine Is Using Elon Musk's Starlink for Drone Strikes on Russian Tanks

ALEXANDER FREUND

2022

INTERESTING ENGINEERING

By Chris Young

2025

World's first 6G electronic warfare weapon by China can jam F-35 radar in seconds

Researchers claim the new 6G system is capable of jamming US F-35 stealth fighter jet radars.

Lloyd's List

Ece Göksedef

2026

War zone GNSS interference surges across the Middle East Gulf

WIRED

MATT BURGESS

Attacks on GPS Spike Amid US and Israeli War on Iran

2026

DEFENCEHQ

Powered By THE TIMES OF INDIA

US brings EA-37B 'Compass Call' to Iran war: The electronic attack jet that can jam communications, blind radar

2026

Next-Generation Cognitive Radar

Benjamin Bloom's Taxonomy [1956] applied to cognitive radar

- Level 1: Prior measurements or databases in radar
- Level 2: Learning-based algorithms for adaptive radar
- Level 3: Knowledge-aided processing for a dynamic scene
- Level 4-6: Higher-order cognition to interconnect, decide, synthesize

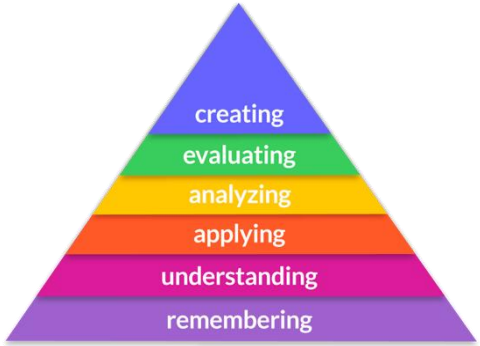

Next-Generation Cognition

- Cognitive Radar: adaptive sensing + optimized processing
- Super-cognition: for legacy radars
- Ultra-cognition: to build cognitive strategy databases
- Hyper-cognition: All submodules operate cognitively

- Metacognition
- Inverse cognition
- Inverse-inverse cognition
- Cognition masking

Inverse Cognition

- Inverse cognition: Counter-adversarial techniques at the target-end
- Design of inverse stochastic filters
- Stability of inverse filters

Adversarial Inference

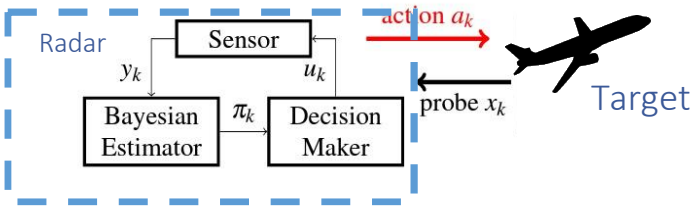

K. V. Mishra, M. R. B. Shankar, and B. Ottersten, "Toward metacognitive radars: Concept and applications," IEEE International Radar Conference, pp. 77-82, 2020.
K. V. Mishra, M. R. B. Shankar, and M. Rangaswamy, "Next-Generation Cognitive Radar Systems," IET Press, 2023

Inverse Cognition

- **Inverse filtering**
  - Radar sends EM pulse, estimates target position from the received signal
  - Radar's action: signal waveform, angular beamforming
  - Target observes radar's action and infers radar's estimate

Radar/them/adversary
Estimates $\hat{x}_k$,
Takes action a_k

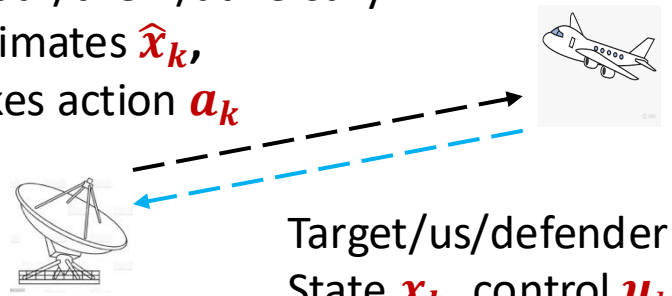

Target/us/defender
State x_k, control u_k,
Estimates $\hat{\hat{x}}_k$

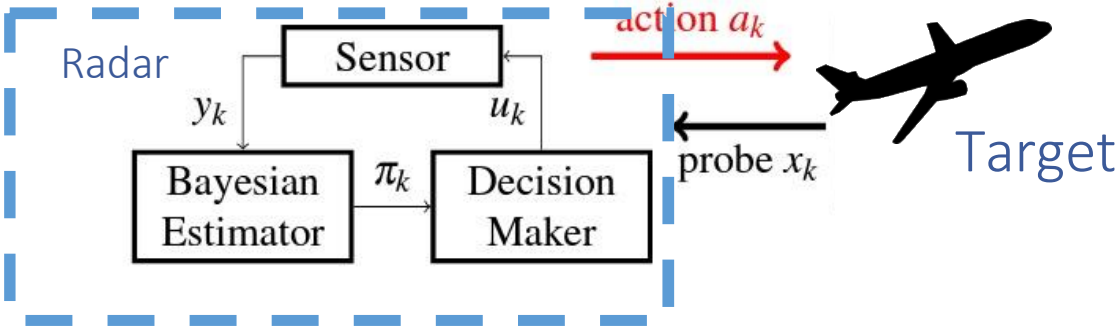

H. Singh, A. Chattopadhyay, and K. V. Mishra, "Inverse extended Kalman filter - Part I: Fundamentals," IEEE T-SP, 2023.
H. Singh, K. V. Mishra and A. Chattopadhyay, "Inverse extended Kalman filter - Part II: Highly non-linear and uncertain systems," IEEE T-SP, 2023.
H. Singh, K. V. Mishra and A. Chattopadhyay, "Inverse unscented Kalman filter," IEEE T-SP, 2024.
H. Singh, K. V. Mishra and A. Chattopadhyay, "Inverse cubature and quadrature Kalman filter," IEEE T-AES 2024.
H. Singh, A. Chattopadhyay and K. V. Mishra, "Inverse particle filter," IEEE T-SP 2025.

Inverse Stochastic Filters

- **Inverse filtering algorithms**
  - Inverse EKF with unknown input
  - Inverse EKF without unknown input
  - Inverse KF with unknown input
  - Gaussian sum EKF
  - Second-order EKF (SOEKF)
  - RKHS-EKF
  - I-UKF, I-CKF, I-QKF
- **Stability analysis**
  - I-EKF without unknown input
  - I-SOEKF
  - I-KF with unknown input
  - I-UKF, I-CKF, I-QKF

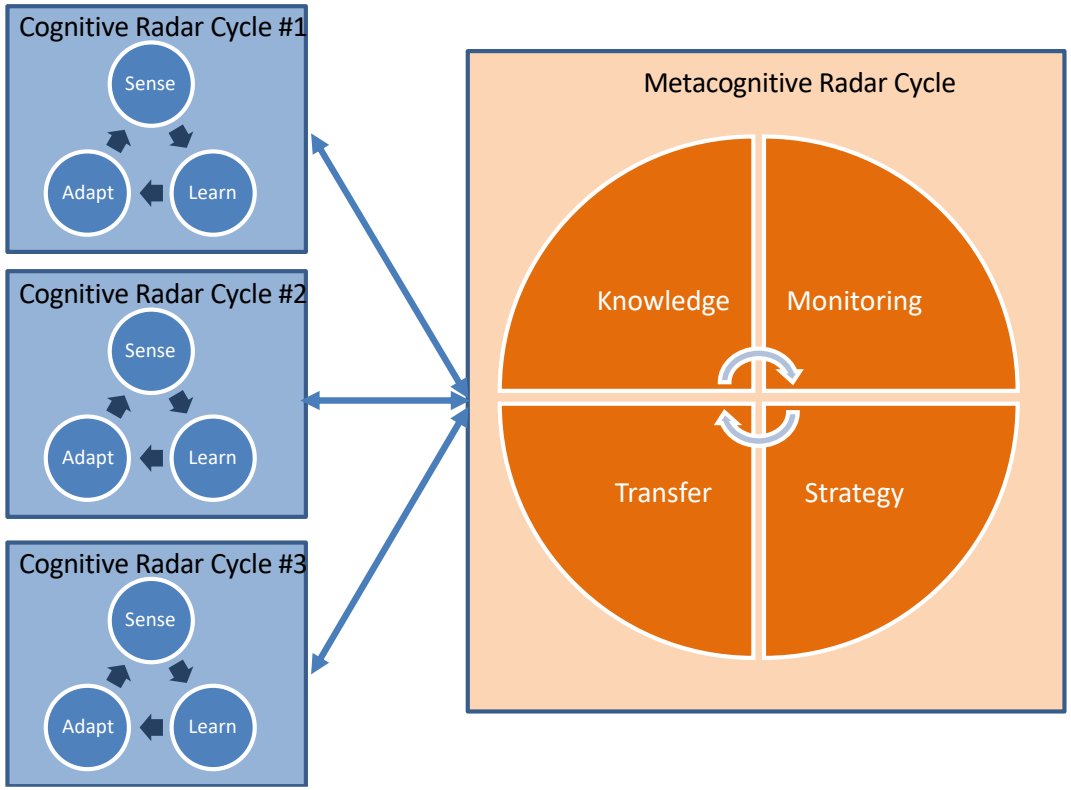

Stability of Inverse Filters

- **Bounded non-linearity approach:** very similar to standard Lyapunov drift-based techniques
  - Hard to establish in our problem
  - Existing work on EKF stability could not establish it completely
  - Reference: Reif et al., IEEE TAC 1999
- **Unknown matrix approach:** Compensates for the effect of nonlinearity induced additive offset in the error dynamics by an unknown matrix multiplication

Theorem (Singh, Chattopadhyay, Mishra, 2023)

Suppose that the one step prediction forward EKF is stable as per Reif et al. 1999. Let the following assumptions additionally hold true:

1. There exist positive real number bounds such that for all $k \geq 0$, the following bounds hold: $\epsilon_l \boldsymbol{I} \preccurlyeq \bar{\boldsymbol{R}}_k \preccurlyeq \epsilon_u \boldsymbol{I}, m_l \boldsymbol{I} \preccurlyeq \bar{\boldsymbol{\Sigma}}_k \preccurlyeq m_u \boldsymbol{I}, ||\boldsymbol{G}_k|| \leq \bar{g}$
2. $\boldsymbol{H}_k$ is full column rank for every k
3. There exist suitable positive constants such that, $\left|\left|\bar{\chi}(\hat{\boldsymbol{x}}, \hat{\hat{\boldsymbol{x}}})\right|\right|_2 \leq \kappa_{\bar{\chi}} ||\hat{\boldsymbol{x}} - \hat{\hat{\boldsymbol{x}}}||_2^{\,2}$ for $\left|\left|\hat{\boldsymbol{x}} - \hat{\hat{\boldsymbol{x}}}\right|\right| \leq \epsilon_{\bar{\chi}}$ (bounded non-linearity)

Then the error process of the inverse EKF is exponentially bounded in the mean square sense and with probability one, provided that the estimation error is always bounded within a suitable ϵ ball

Courtesy: Independence Day (1998)

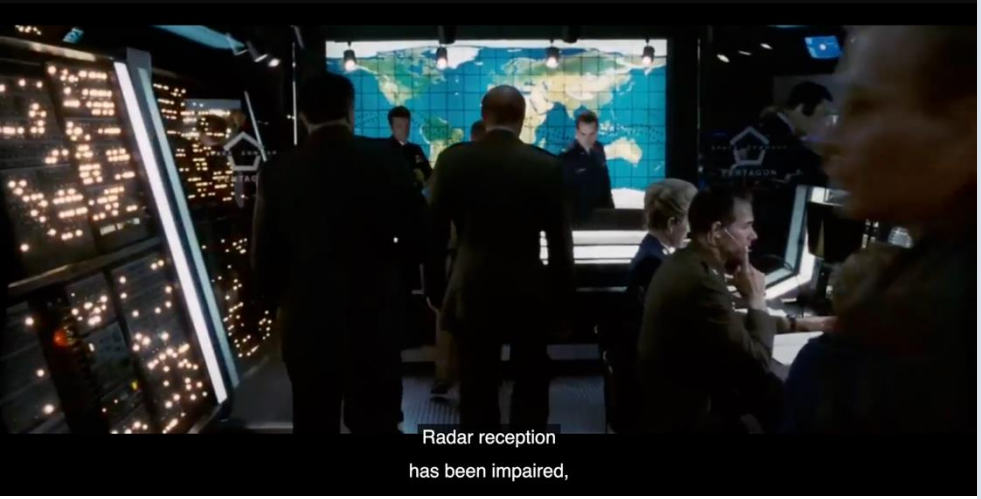

Other EW Applications of ISAC

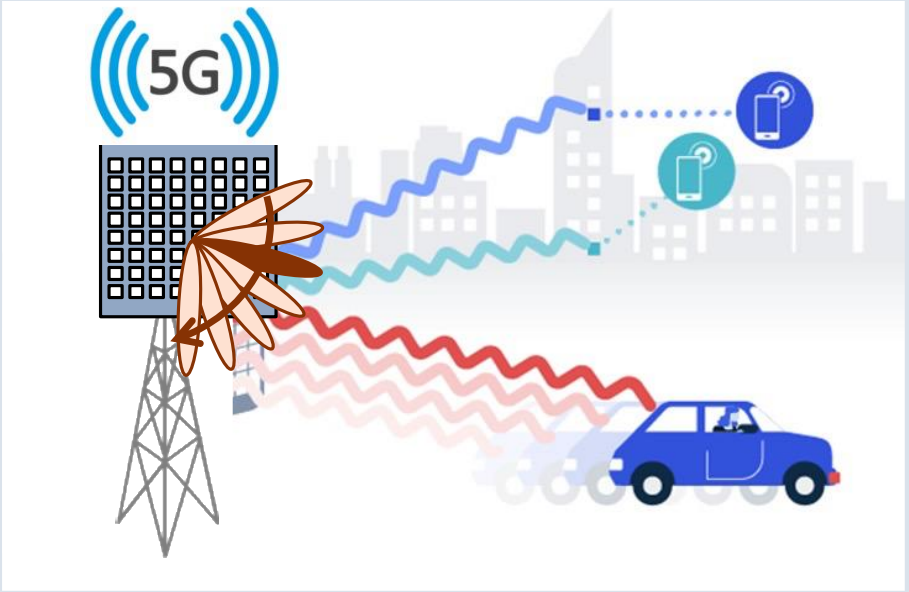

Dual-Blind Deconvolution

Multi-antenna receiver

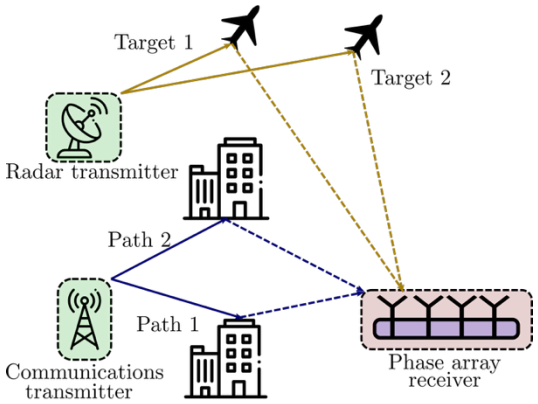

n-tuple BD

- SDP formulation

$$\underset{\mathbf{q},\mathbf{Q}}{\text{maximize}} < \mathbf{q},\mathbf{y} >_{\mathbb{R}} \text{ subject to}$$

$$\begin{bmatrix} Q & \tilde{Q}_{r_1}^H \\ \tilde{Q}_{r_1} & I_J \end{bmatrix} \succcurlyeq 0, \begin{bmatrix} Q & \tilde{Q}_{c_1}^H \\ \tilde{Q}_{c_1} & \mu_c I_{PJ} \end{bmatrix} \succcurlyeq 0,$$

$$\vdots$$

$$\begin{bmatrix} Q & \tilde{Q}_{r_{K_r}}^H \\ \tilde{Q}_{r_{K_r}} & I_J \end{bmatrix} \succcurlyeq 0, \begin{bmatrix} Q & \tilde{Q}_{c_{K_c}}^H \\ \tilde{Q}_{c_{K_c}} & \mu_c I_{PJ} \end{bmatrix} \succcurlyeq 0$$

$$\text{Tr}(\boldsymbol{\Theta}_n \mathbf{Q}) = 0$$

Unsynchronized transmission

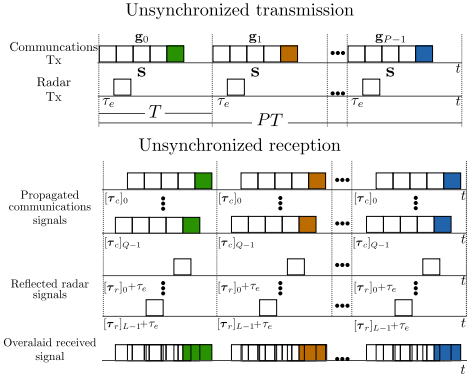

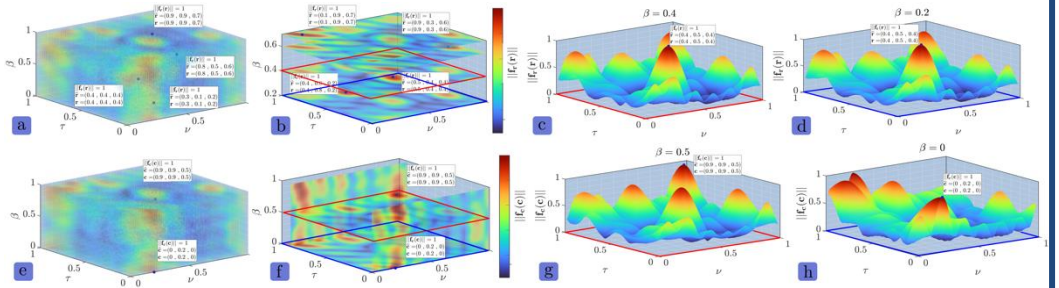

Low-rank Hankel-type Matrix recovery

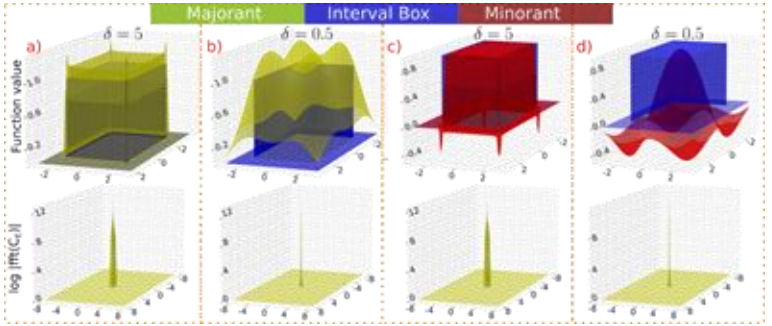

R. Jacome, E. Vargas, K. V. Mishra, B. M. Sadler and H. Arguello, "Multi-antenna dual-blind deconvolution for joint radar-communications via SOMAN minimization." Signal Processing, 2024.

E. Vargas, K. V. Mishra, R. Jacome, B. M. Sadler and H. Arguello, "Joint radar-communications processing from a dual-blind deconvolution perspective," IEEE ICASSP, 2022.

J. Monsalve, E. Vargas, K. V. Mishra, B. M. Sadler and H. Arguello, "Dual-blind deconvolution in ISAC receiver using multi-dimensional Beurling-Selberg functions," RadarConf 2024

Opportunistic ISAC using 5G Base-Stations

Full-Duplex BS for Weather Sensing

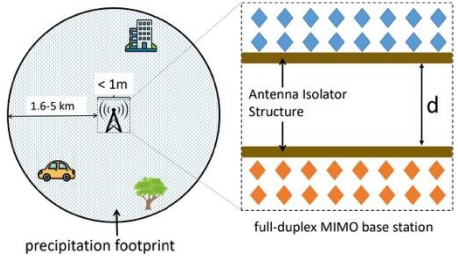

(a) view from the base station

(b) base station configuration

5G BS-Based Aerial Radar Detection

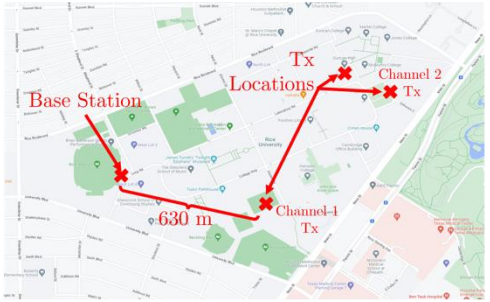

SINC: Synergistic Imaging and Comms

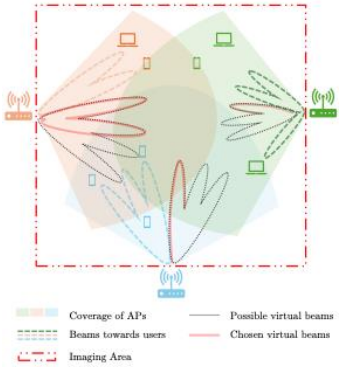

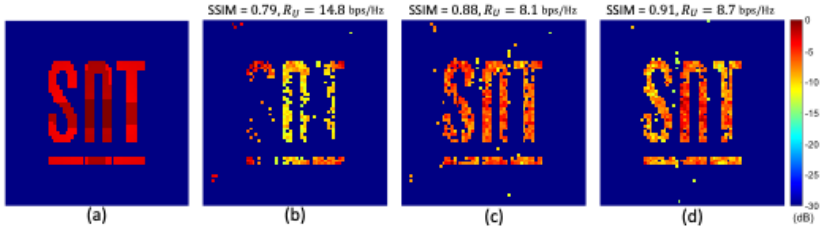

Z Chen, KV Mishra, D Pandey, A Sabharwal, “Near-ground Precipitation Sensing Using Full-duplex MIMO Base Stations,” IEEE J-STEAP, 2025.

N. Raymondi, K. V. Mishra, A. Sabharwal, “Detecting aerial radars from massive MIMO base-stations: Design and experimental evaluation," IEEE T-AES, 2026.

A. Murtada, K. V. Mishra, M. R. B. Shankar, “SINC: Synergistic imaging and communications via distributed MU-MIMO," IEEE SSP, 2025.

Courtesy: The Plot Against America (Part 3)

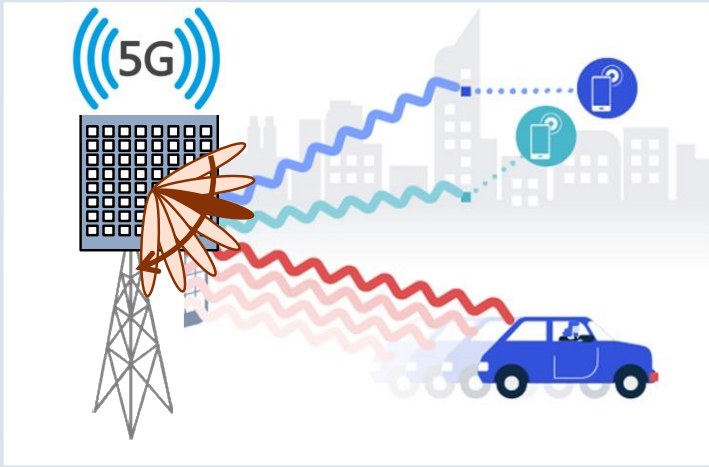

More Information

Thank you!

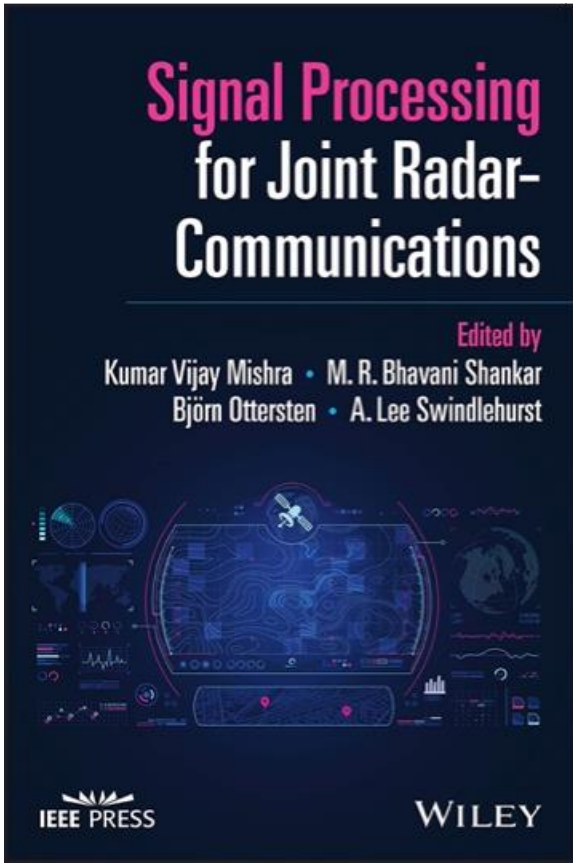

Special Mention: 2025 Wiley-IEEE Press Professional Book Award

LinkedIn https://www.linkedin.com/in/vizziee/

2024 IEEE SPS Pierre-Simon Laplace Early Career Technical Achievement Award
"for major contributions in radar signal processing and the integration of sensing and communications"

2025 SAE International Award for Excellence in Innovation
"in emerging technologies across the mobility industry"